International Journal of Science and Research (IJSR)
ISSN: 2319-7064
SJIF (2022): 7.942

New Insights into the Nanocomposite Composition of TiO_2-Ag-TEOS-La for Photocatalytic Applications

Roghaiyeh Mazloumihaghghi[1], Saeidreza Pournaghshband[2], Yaser Talaeiramsheh[3]

[1*] Department of Agricultural and Mechanical Engineering, Science and Research Branch, Islamic Azad University, Tehran, Iran
[1]Email: *roghaiyeh.mazloumihaghghi[at]yahoo.com*

[2] Quality Control of Nasozgozarpardazi, Ir8153956841, Tabriz, Iran

[3]Department of Materials Engineering, Tabriz Branch, Islamic Azad University, Tabriz, Iran

Abstract: ***Nanotechnology is one of the most important of these technologies, whose applications are associated with lower energy consumption, and better properties. The best way to clean contaminated sites is to use a photocatalyst that is suitable for a large number of pollutants.In this study, a TiO_2-Ag-TEOS-La nanocomposite was synthesized as a degradation product and photocatalyst by the sol-gel method. The samples were calcined and then XRD, FTIR, FESEM, and analyzes were used to characterize the synthesized powders. In addition, a UV-Vis was used to study the absorption of composite. The degradation and photocatalytic test of nanocomposites were investigated on methylene blue dye. The results of the experiments show us that the nanocomposite has the best performance in the role of environment and the amount of a concentration of methylene blue and finally has 88% destruction.***

Keywords: Nanotechnology; Sol-gel; Photocatalyst; XRD; FTIR

1. Introduction

Nanotechnology is one of the most important of these technologies, whose applications are associated with lower costs, longer life, lower energy consumption, lower maintenance costs and better properties[1]. The best way to clean polluted places is to use a photocatalyst, which is suitable for a large number of pollutants. In recent decades, the economic and technological importance of photocatalysts has increased considerably. Photocatalysts are catalysts that are activated by light and convert pollutants in the air or water into less harmful substances such as water and carbon dioxide[2],[3]. From the use of photocatalysts in the production of vapor repellent, antimicrobial and self-cleaning surfaces to water and air purification and hydrogen production using solar energy, they have all found their way to commercialization[4]. Among all available photocatalysts, titanium oxide (TiO_2) was chosen due to its high stability, non-toxicity and availability, its high photochemical properties and its corrosion resistance[5]. The band gap of titania (3 eV for the rutile phase and 3.2 eV for the anatase phase) is in the ultraviolet region, which represents less than 10 % of the solar energy. In addition to this obstacle, the high rate of electron-hole rearrangement limits the application of these particles[6]. One way of solving these problems and increasing efficiency and photocatalytic activity is by doping titanium dioxide with precious and transition metals platinum, copper, silver[7]. The doping of elements into the titanium dioxide lattice has brought about important steps in the field of band gap technology and the optical reaction of semiconductors[8]. The main goal of doping is to reduce the band gap or to introduce new energy levels into the band gap, allowing the semiconductors to absorb visible light[9]. The main goal of this research is the doping of silver and lanthanum elements into the crystal lattice of titanium dioxide. In this study, the synthesis and characterization of TiO2-Ag-TEOS-La nanoparticles and their photocatalytic properties were investigated.

2. Experimental Equipment and Materials

All precursors were prepared by Merck. To perform the procedure, colored solutions were prepared at different concentrations from 5 to 40 mg/L by diluting the 300 mg/L solution with distilled water. Then their calibration curve was established by measuring the absorbance of UV light. To measure the absorbance of the samples, various tests were performed and the effects of different parameters on the color absorbance of the samples were investigated. In this experiment, the effects of calcination temperature for optimal composite synthesis, the effect of pH, the effect of color concentration, the selection of the optimal amount of powder used and the effect of time were investigated, which are explained below. The basis of the work is that 0.05 gram of each powder was placed in 30 ml of methylene blue solution with a concentration of 30 ppm with different pH and stirred with a magnetic stirrer under UV light, and then placed in a centrifuge, and at different times, an amount of it was separated from the solution and its degradation and absorption rate were measured in the UV-Vis spectrophotometer. The phase series was confirmed by X-ray diffraction (XRD) and a Philips XRD diffractometer with $Cu_{k\alpha}$ radiation at 40 KV, 30 mA, a step size of 0.05^{o} (2Θ) and a scan rate of 1^{o}/min and X'Pert software was used for qualitative analysis and report of width diffraction peaks (rad, β) at full width half maximum (FWHM) in different 2θ values according to the situation of peaks (Version 4.9.0).Absorption spectra were also registered using AvaSpec-ULS2048XL-EVO and AvaSoft 8.

3. Synthesize and methods

The general process of synthesizing nanoparticles in this research is as follows. First, 50 ml of 2-propanol was poured into the beaker, then 1 gram of lanthanum nitrate was added and the sample was stirred for 1 hr. After the lanthanum nitrate has completely dissolved and the solution is clear, 0.02 g of silver nitrate and 1 ml tetraethyl orthosilicate (TEOS) is added and the solution is stirred again for 1 hr. After the above time has elapsed and the silver nitrate has completely dissolved and the solution has become homogeneous, titanium isopropoxide is slowly added to the solution in an amount of 13 ml and distilled water is added dropwise after 30 minutes. The drop is added slowly and the solution is given the opportunity to form a gel. After the gel has formed, the solvent is removed by raising the temperature of the stirrer to 120 degrees Celsius, the boiling and evaporation temperature of the solvent, and the gel is obtained in the form of powder. Then the powder is washed twice with distilled water and filtered, then it is poured into cans and put into the dryer for drying for 24 hours at a temperature of 150 degrees Celsius. After drying for calcination in the oven with air atmosphere and with a heating rate of 50 °C/min, calcination was carried out at a temperature of 650°C. In this experiment, nanocomposites with the compositions shown in Table 1.

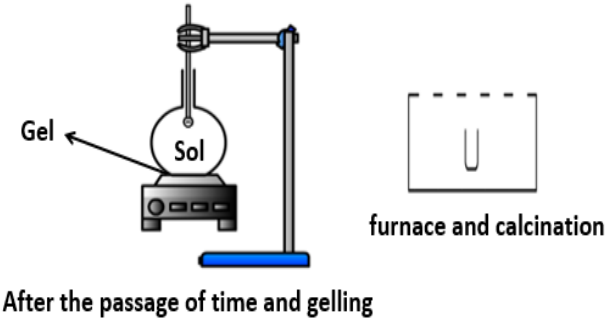

Figure 1: The schematic of synthesis nanocomposite

Table 1: The composition of composites

Composite	TiO_2 (wt.%)	La (wt.%)	TEOS (wt.%)	Ag (wt.%)
TiO_2-La-TEOS-Ag	84	10	1	5

4. Result and Discussions

4.1 X-ray diffraction

Figure 2 shows the X-ray diffraction analyzes of the samples. As can be seen in XRD pattern, the desired phases are formed in all stoichiometry of the synthesized nanocomposites without additional peaks, and the intensity of the corresponding peaks decreases with the reduction of the titanium dioxide content. The titanium dioxide phase is anatase[10],[11], and the sharp peaks are associated with it.

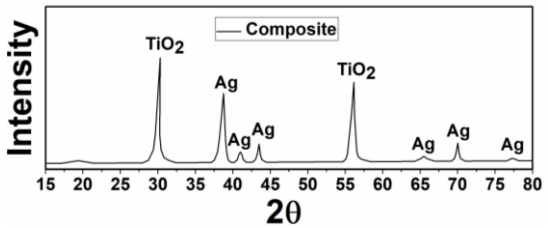

Figure 2: XRD spectra of composite

4.2 FTIR

In the FTIR spectrum (**Figure 3**), each peak represents the absorption in the corresponding wavenumber and is characterized by a chemical bond. Consequently, the wavenumber of each peak indicates the presence of a specific functional group in the sample[12]. In general, the more polar a bond is, the higher the absorption rate and the higher the peak. Range of group frequencies: This region is in the range of 1200-1400 cm^{-1}, and the peaks in this region are undoubtedly associated with a particular functional group, considering that the peak is associated with each group[13]. A factor is located in a small and specific region, the presence of this group of factors can be detected in the sample. The overall structure of the molecules is deduced and used only to confirm the proposed structure[14].As can be seen from FTIR spectra, despite washing the samples, the resulting peaks indicate the presence of residual raw materials in the synthesized powders, however, after calcination, many compositions have been removed or reduced.

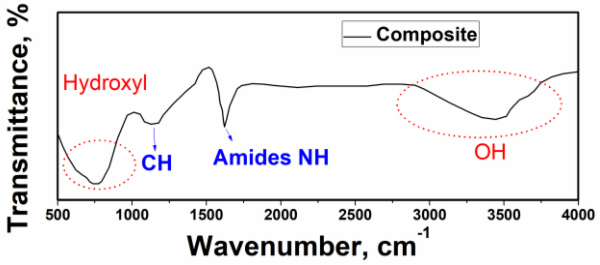

Figure 3: FTIR spectrum of composite

4.3 Absorption analysis

Figure 4 shows the absorption spectra of the coated composite on top of the solid fil. The maximum wavelength is about 325 nm, which is in the non-visible range due to the TiO_2 content in the synthesized composite[15]. In addition, the effect of TEOS is clear when the broad band from 400 to 530 nm is observed. The intermolecular charge transfer is also dominated in this region and the lower optical band gap [16]of about 1.79 eV is calculated, which is advantageous for the photocatalytic application of this type of composite.

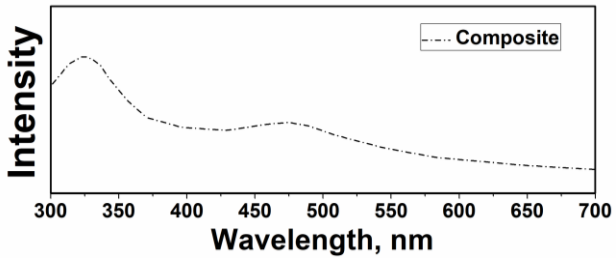

Figure 4: Absorption spectra of coated composite on the top of film

4.4. Degradation test and photocatalytic properties

To investigate the optimal type of composite, solution of 10 ppm methylene blue with a pH of 9, 0.1 M NaOH and first stirred for 5 minutes in a dark room with the UV lamp off. Then the UV lamp was turned on and the results of the destruction were performed. As it can be seen that the amount of composite shows well result as the surface area is reduced for larger amounts with agglomerated particles and thus the degree of destruction is also lower[17].To investigate the performance of dye degradation in three acidic, neutral and alkaline environments, 0.1 M NaOH and HCl were used to adjust the pH. Three solutions of 10 ppm methylene blue with pH values of 2, 5 and 7 were prepared and 0.1 g of the nanocomposite was added. According to the degradation result, it can be concluded that the destruction occurs better in the play environment, as a negative charge is generated on the surface of the play environment, which can bring the color closer to itself and perform the destruction operation faster, as the destruction occurs in the interstices very close to the surface[18],[19].To ensure non-absorption of methylene blue by the nanocomposites, the absorption test was performed under optimal conditions in the absence of light[20]. The results showed that the sample tested in the absence of light as an absorbent had an absorbance of 26% under the same optimal conditions and in a period of 1 hr., compared to the same sample in the presence of UV light, which has a photocatalytic activity of 88%. It can be concluded that the prepared sample was not efficient in the absorption process and can only be expected to have high activity as a photocatalyst in the degradation process.In general, it can be said that the increase in photocatalytic activity occurs under optimal and identical conditions for composite due tothe existence of Si derivative (TEOS), lanthanum and silver ions in the photocatalyst structure, which decreases the energy of the band gap and also generates more electron-hole pairs. Furthermore, increasing the amount of doping prevents the growth of titanium oxide particles, which increases the specific surface area[21]. On the other hand, the shrinking of the particles leads to a rapid transfer of electron holes to the surface and thus prevents their rapid unification.

5. Conclusions

In this study, a nanocomposite was synthesized by sol-gel method with considering calcination temperature with a particle size less than 100 nanometers due to the XRD pattern. This result demonstrates the controllability of the sol-gel method and the proposed system able to form the desired composite nanoparticles. Particles synthesized by sol-gel method have a suitable surface charge in the play environment, which made the nanocomposites a strong destroyer of the cationic methylene blue dye. The synthesized particles have good photocatalytic properties, which is due to the narrowing and narrowing of the band gap of titanium dioxide (2.7 eV) by simultaneous doping with silver, TEOS and lanthanum, and it causes more electron-hole production. The electron holes produced move in opposite directions, which prevents them from bonding quickly. The best photocatalytic activity at an optimal concentration of the pollutant model, at a basic pH and an amount of 0.1 grams of the powder composite was selected as the optimum amount for degradation. From the degradation results in the photocatalyst optimization test, it can be concluded that increasing the amount of photocatalyst from the optimum limit due to the turbidity of the sample not only improves but also reduces the degradation process.

Acknowledgements
The authors would like to thank Nasozgozarpardazi for coverage and support.

References

[1] Radzi, A. (2023) The Ruhr innovation ecosystem—From industrial brownfields to regenerative smart environments. *Intell. Environ. Adv. Syst. a Heal. Planet, Second Ed.*, 33–85.
[2] Liu, J., Zhang, S., Wang, W., and Zhang, H. (2023) Photoelectrocatalytic principles for meaningfully studying photocatalyst properties and photocatalysis processes: From fundamental theory to environmental applications. *J. Energy Chem.*, **86**, 84–117.
[3] Saka, C., and Balbay, A. (2020) Influence of process parameters on enhanced hydrogen evolution from alcoholysis of sodium borohydride with a boric acid catalyst. *Int. J. Hydrogen Energy*, **45** (32), 16193–16200.
[4] Wu, C., Wu, F., Bai, Y., Yi, B., and Zhang, H. (2005) Cobalt boride catalysts for hydrogen generation from alkaline NaBH4 solution. *Mater. Lett.*, **59** (14–15), 1748–1751.
[5] Dai, H., Cai, X., Li, X., Wang, C., Hou, Y., and Wei, R. (2023) First-principles calculations on performance of the g-C3N4/LNS-TiO2(Cr+C) heterojunction photocatalyst in water splitting process. *Int. J. Hydrogen Energy*, **48** (98), 38742–38748.
[6] Huang, J., Song, H., Chen, C., Yang, Y., Xu, N., Ji, X., Li, C., and You, J.A. (2017) Facile synthesis of N-doped TiO2 nanoparticles caged in MIL-100(Fe) for photocatalytic degradation of organic dyes under visible light irradiation. *J. Environ. Chem. Eng.*, **5** (3), 2579–2585.
[7] Ma, J., Liu, Q., Zhu, L., Zou, J., Wang, K., Yang, M., and Komarneni, S. (2016) Visible light photocatalytic activity enhancement of Ag3PO4 dispersed on exfoliated bentonite for degradation of rhodamine B. *Appl. Catal. B*

Environ., **182**, 26–32.

[8] Saka, C. (2023) Metal-free hybrid composite particles with phosphorus and oxygen-doped graphitic carbon nitride dispersed on kaolin for catalytic activity toward efficient hydrogen release. *Int. J. Hydrogen Energy*, **48** (37), 13864–13876.

[9] Loghmani, M.H., and Shojaei, A.F. (2014) Hydrogen production through hydrolysis of sodium borohydride: Oleic acid stabilized Co–La–Zr–B nanoparticle as a novel catalyst. *Energy*, **68**, 152–159.

[10] Abdul Rahim, N., Rosdzimin Abdul Rahman, M., Amali Bin Ahmad, K., Rahim Mat Sarip, A., Hasbullah, S., and Suhel, A. (2023) Analysis of waste cooking oil biodiesel (WCO) synthesis with TiO2 impregnated CaO from waste shells nano-catalyst. *Mater. Today Proc.*

[11] Gardy, J., Hassanpour, A., Lai, X., Ahmed, M.H., and Rehan, M. (2017) Biodiesel production from used cooking oil using a novel surface functionalised TiO2 nano-catalyst. *Appl. Catal. B Environ.*, **207**, 297–310.

[12] Oto, B., Gulebaglan, S.E., Madak, Z., and Kavaz, E. (2019) Effective atomic numbers, electron densities and gamma rays buildup factors of inorganic metal halide cubic perovskites CsBX3 (B = Sn, Ge; X = I, Br, Cl). *Radiat. Phys. Chem.*, **159**, 195–206.

[13] Kara, U., Kavaz, E., Issa, S.A.M., Rashad, M., Abuzaid, M.M., Erdemir, R.U., and Tekin, H.O. (2020) FTIR, structural and radiation attenuation properties of amalgam dental composites for medical applications. *Mater. Chem. Phys.*, **253**, 123261.

[14] Wang, W., Wang, Y., Zhao, X., Li, Y., He, H., Lian, L., Zeng, K., Wu, L., Deng, L., and Liu, Y.-N. (2024) Surface oxygen vacancies of TiO2–x enabled water transfer photocatalytic hydrogenation of nitrobenzene to aniline without use of co-catalyst. *Chem. Eng. Sci.*, **285**, 119645.

[15] Jia, G., Wang, Y., Cui, X., Zhang, H., Zhao, J., Li, L.H., Gu, L., Zhang, Q., Zheng, L., Wu, J., Wu, Q., Singh, D.J., Li, W., Zhang, L., and Zheng, W. (2022) Wet-chemistry hydrogen doped TiO2 with switchable defects control for photocatalytic hydrogen evolution. *Matter*, **5** (1), 206–218.

[16] Li, M., Guo, Q., and Nutt, S. (2017) Carbon nanotube/paraffin/montmorillonite composite phase change material for thermal energy storage. *Sol. Energy*, **146**, 1–7.

[17] Campa, M.C., Fierro, G., Doyle, A.M., Tuti, S., Catracchia, C., and Pietrogiacomi, D. (2023) Combined use of in situ and operando-FTIR, TPR and FESEM techniques to investigate the surface species along the simultaneous abatement of N2O and NO on Pt,Pd,Rh/TiO2-ZrO2 and Pt,Pd,Rh/TiO2-ZrO2-CeO2 catalysts. *Surfaces and Interfaces*, **42**, 103502.

[18] Shan, W., and Song, H. (2015) Catalysts for the selective catalytic reduction of NOx with NH3 at low temperature. *Catal. Sci. Technol.*, **5** (9), 4280–4288.

[19] Zhao, L., Wang, H. xiao, Xu, M. xin, Liu, Z. shu, and Lu, Q. (2021) Simultaneous removal of NO and N2O over commercial V2O5-MoO3/TiO2 catalyst modified with bismuth-nickel oxides. *Appl. Catal. A Gen.*, **625**, 118336.

[20] McKenna, F.M., and Anderson, J.A. (2011) Selectivity enhancement in acetylene hydrogenation over diphenyl sulphide-modified Pd/TiO2 catalysts. *J. Catal.*, **281** (2), 231–240.

[21] Shao, X., Guo, X., Shi, X., Wang, B., Fan, M., and Zhang, R. (2024) C2H2 semi-hydrogenation over Pdn/TiO2 and PdnCO/TiO2 catalysts: Probing into the roles of Pd cluster size and pre-adsorbed CO in tuning catalytic performance. *Fuel*, **358**, 130053.